A Comparison of Strategies for Obtaining High-Resolution NMR Spectra of Quadrupolar Nuclei *

R. E. Youngman, U. Werner-Zwanziger, and J. W. Zwanziger
Department of Chemistry, Indiana University, Bloomington, IN 47405

Z. Naturforsch. **51a**, 321–329 (1996); received October 10, 1995

A comparison of high-resolution NMR methods for quadrupolar nuclei is presented. The samples studied are pure and modified boron oxide glasses, and the boron NMR spectra are recorded using three different experiments capable of high resolution: Double Rotation, Dynamic Angle Spinning, and Multiple-Quantum Magic Angle Spinning. Resolution of the similar ring and nonring boron sites in these glasses, in the presence of disorder, provides a realistic study of the strengths and limitations of these experiments. Conclusions about the relative applicability of these experiments in different situations are presented.

1. Introduction

The nuclear quadrupole interaction (NQI) reflects the coupling between the nuclear quadrupole moment and the electric field gradient at the nucleus. The electric field gradient contains information about the local electron distribution, and as such the NQI is a rich source of information on the structure of solid materials. Because the majority of elements in the periodic table have non-zero quadrupole moments, measuring this interaction precisely is of continuing interest. In the present paper we will compare several recently developed NMR experiments which can yield such precise measurements. The experiments used include Double Rotation (DOR), Dynamic Angle Spinning (DAS), and Multiple-Quantum Magic Angle Spinning (MQ-MAS).

The results presented here are on borate glasses, in particular on boron-11 (spin 3/2, $eQ = 3.55 \times 10^{-30}\,\mathrm{m}^2$). For this paper our aim was not to show samples that give the narrowest possible lines, although the differences in this quantity between different experiments is interesting in its own right; rather we chose samples that exhibit some disorder and thereby provide a test of the methods under conditions that more accurately reflect those typically encountered by solid state scientists. In so doing we present the first applications of DOR and MQ-MAS to borate glasses, and the first high-resolution NMR results on potassium borate glasses.

The focus of the paper is a critical comparison of the different methods, including both their information content and ease of use. In the next section we briefly outline the relevant theory, and motivate the different methods. Then we discuss in more detail the implementation of each method, as we have used them in our laboratory. We then present results, and discuss their use and meaning. Finally we conclude with comments on the relative applicability of the different approaches.

2. Theory

The theory of NMR experiments designed for quadrupolar nuclei has been reviewed (see for example [1]). Our purpose here is to provide a very brief outline, in order to motivate the different experiments used.

If magnetic fields of arbitrarily large strength were available, the quadrupole interaction could be fully truncated by the Zeeman interaction, and the remaining broadening removed by magic angle spinning. For many nuclei, however, existing magnetic fields are too weak for complete truncation, and effects that are second order in the quadrupole interaction are important. This is typically the case for nuclei such as ^{17}O, ^{11}B, etc. The Hamiltonian can be expanded as [2]

$$H = H_Z + H_{CS} + H_Q^{(1)} + H_Q^{(2)}, \qquad (1)$$

* Presented at the XIIIth International Symposium on Nuclear Quadrupole Interactions, Providence Rhode Island, USA, July 23–28, 1995.

Reprint requests to Prof. J. W. Zwanziger.

0932-0784 / 96 / 0500-0321 $ 06.00 © – Verlag der Zeitschrift für Naturforschung, D-72072 Tübingen

where H_Z is the Zeeman Hamiltonian, H_{CS} is the chemical shift, and H_Q is the quadrupole Hamiltonian, expanded with perturbation theory to second order. The terms of the quadrupole Hamiltonian take the form (in frequency units)

$$H_Q^{(1)} = \omega_Q R_{2,0} T_{2,0}, \tag{2}$$

$$H_Q^{(2)} = \frac{\omega_Q^2}{\omega_Z} \sum_{m=1}^{2} \frac{R_{2,m} R_{2,-m} [T_{2,-m}, T_{2,m}]}{m}. \tag{3}$$

Here ω_Z is the Larmor frequency and ω_Q is the quadrupole coupling constant,

$$\omega_Q = \frac{2\pi (e^2 Q q/h)}{2I(2I-1)} \tag{4}$$

for a nucleus of spin I and quadrupole interaction $e^2 Q q/h$. The transformation from the quadrupole principal axis frame to the laboratory frame is effected by a second rank spherical tensor with components $R_{2,m}$, and the dependence of the quadrupole interaction on spin variables is given by the second rank spherical tensor with components $T_{2,m}$. Both of these tensors are described, for example, by Haeberlen [3].

Except for the $|I, \frac{1}{2}\rangle \leftrightarrow |I, -\frac{1}{2}\rangle$ (central) transition, on which it has no influence, the first-order quadrupole broadening (Eq. (2)) results in single-quantum transitions that are hundreds to thousands of kHz wide in typical cases. The first-order broadening can be removed by magic angle spinning due to its pure rank-2 spatial dependence. This fact is the basis of the satellite transition spectroscopy (SATRAS) method [4, 5], which allows the resolution of sites with differing quadrupole interactions. Second-order broadenings (3) remain, however, making lineshape simulations necessary to extract the quadrupole coupling and chemical shift parameters. In this paper we focus on techniques that remove all anisotropic interactions through second order.

The central transition itself is unaffected by quadrupole interactions in first order, but is broadened by the second-order term (3). As explained elsewhere [1, 2], the tensors in (3) can be recoupled with Clebsch-Gordan series, yielding rank-1 and rank-3 spin tensors and rank-0, rank-2, and rank-4 space tensors. The rank-0 term gives an isotropic shift due to the quadrupole coupling. Measuring this shift accurately is the most precise way of determining the quadrupole interaction from NMR experiments.

The spectral broadening of the second order quadrupole perturbation term arises from the rank-2 and rank-4 spatial tensors. These can be modulated by rotating the sample during the experiment; the result, in the fast spinning limit, is a spatial dependence of the form [1]

$$a_0 + a_2(\theta, \phi)\, P_2(\cos\beta) + a_4(\theta, \phi)\, P_4(\cos\beta), \tag{5}$$

where $P_l(\cos\beta)$ is a Legendre polynomial of $\cos\beta$, where β is the angle between the rotor axis and the magnetic field; a_0 is a constant; and a_2 and a_4 are functions of the angles θ and ϕ relating the quadrupole principal axis system to a rotor-fixed frame. The rank-2 spatial dependence $P_2(\cos\beta)$ is removed by conventional magic angle spinning. The rank-4 term prevents MAS from being completely effective for second-order quadrupole broadening.

No single angle β is sufficient to average (5) to its isotropic part. The most direct averaging method is Double Rotation (DOR), in which a sample is rotated about a continuously moving axis [6–8]. This is accomplished by rotating the so-called outer rotor (see Fig. 1) about an axis at the usual magic angle (that is, where $P_2(\cos\beta) = 0$) with respect to the magnetic field; inside the outer rotor is the sample holder (the inner rotor), which rotates independently about an axis inclined at an angle with respect to the outer rotor axis which is a zero of P_4. The pulse sequence used is just a simple pulse-aquire, as in conventional magic angle spinning. The shifts of the peaks in this experiment include contributions from the isotropic chemical shift and the isotropic portion of the second order quadrupole interaction, and are expressed in ppm as

$$\delta_{iso}^{DOR/DAS} = C_{CS}^{DOR/DAS}\, \delta_{CS} + C_{Quad}^{DOR/DAS} \frac{(e^2 q Q/h)^2}{\nu_0^2} \left(1 + \frac{\eta^2}{3}\right), \tag{6}$$

for isotropic chemical shift δ_{CS}, quadrupole coupling $e^2 q Q/h$ (in MHz) and asymmetry η, and Larmor frequency ν_0 (also in MHz). The coefficients are given in Table 1, and depend on spin for the quadrupole portion.

Less direct than DOR, but mechanically easier to implement, is Dynamic Angle Spinning (DAS) [9–11]. Here the sample rotates about one axis during part of the experiment; the axis is then switched to a second axis just prior to acquisition. Neither rotation axis angle corresponds to zeros of P_2 or P_4. The axes are chosen such that both functions undergo changes in sign between the two angles, enabling a refocussing during evolution at the second angle of the anisotropy

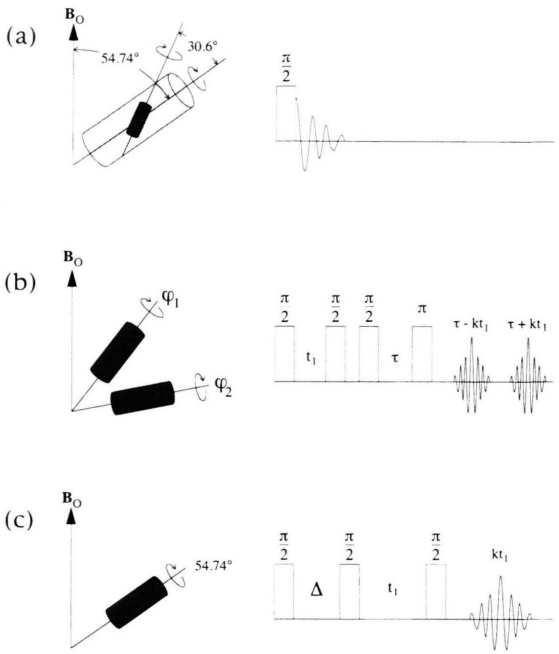

Fig. 1. Sample orientation and pulse sequences used in (a) double rotation (DOR), (b) dynamic angle spinning (DAS), and (c) multiple quantum magic angle spinning (MQ-MAS). In DOR the rotor axis angles are zeros of the second and fourth order Legendre polynomials, $P_2(\cos\beta)=0$ and $P_4(\cos\beta)=0$. For DAS the angles are chosen such that $P_2(\cos\varphi_1)=-kP_2(\cos\varphi_2)$ and $P_4(\cos\varphi_1)=-kP_4(\cos\varphi_2)$. We use $\varphi_1=37.38°$ and $\varphi_2=79.19°$, for which $k=1$. The DAS echo and antiecho form at $\tau\pm kt_1$, and τ is chosen large enough to ensure acquisition of both echoes for all times t_1 used. In MQ-MAS the isotropic echo forms at kt_1, where the value of k is determined by the spin tensor matrix elements. For spin-3/2 it has the value $k=7/9$.

Table 1. Coefficients on the contributions to the isotropic shift, (6) and (7), for DOR, DAS, and MQ-MAS of spin-3/2 and spin-5/2 nuclei. C_{CS} is the coefficient of the chemical shift, and C_{Quad} is the coefficient of the second order quadrupole shift.

Spin	DOR/DAS		MQ-MAS	
	$C_{CS}^{DOR/DAS}$	$C_{Quad}^{DOR/DAS}$	$C_{CS}^{MQ\text{-}MAS}$	$C_{Quad}^{MQ\text{-}MAS}$
3/2	1	−25000	$\frac{17}{8}$	31250
5/2	1	− 6000	$-\frac{17}{31}$	$-\frac{60000}{31}$

acquired at the first angle. DAS is typically implemented as a two-dimensional experiment, using more complex pulse sequences than are used in DOR [12]. The peaks in the isotropic dimension of a DAS experiment appear at the shifts given in (6).

The refocussing in DAS is accomplished using the spatial degrees of freedom; it can also be accomplished using the spin degrees of freedom, as shown recently by Frydman and Harwood [13]. The triple-quantum transition $|I,\frac{3}{2}\rangle \leftrightarrow |I,-\frac{3}{2}\rangle$, like the central transition, is unaffected by first-order broadening. In a two-dimensional experiment, a triple-quantum coherence can be prepared and correlated with the central transition, resulting in an isotropic echo similar to that observed with DAS. Unlike DAS, however, the sample rotates about a single, static axis, conveniently chosen to be the magic angle (this variant is called multiple-quantum magic angle spinning, or MQ-MAS). This experiment then can be performed with standard instrumentation [13]. Of the three experiments, it is mechanically the most straight-forward, but has the most complex pulse sequence due to the extensive phase-cycling required. The isotropic peaks in this experiment again include contributions from the chemical shift and quadrupole interaction, and are given by a formula of the same form as (6),

$$\delta_{iso}^{MQ\text{-}MAS} = C_{CS}^{MQ\text{-}MAS}\,\delta_{CS} + C_{Quad}^{MQ\text{-}MAS}\,\frac{(e^2qQ/h)^2}{\nu_0^2}\left(1+\frac{\eta^2}{3}\right), \tag{7}$$

but with different numerical values for the coefficients (see Table 1).

In the following section we describe how these experiments were implemented to study borate glasses.

3. Experimental Methods

3.1. Sample Preparation

Vitreous B_2O_3 was prepared by dehydrating boric acid in a platinum crucible for one hour at 1000 °C. Glassy samples with natural abundance ^{11}B were made using high purity (99.9995%) boric acid (Strem Chemicals). Samples with boron-10 enrichment were made by combining high-purity boric acid enriched to 97% in ^{10}B (Aldrich) with natural abundance boric acid. Potassium borate glasses with 90% boron-10 enrichment were made by fusing the appropriate amounts of boric acid and potassium carbonate (Strem) at 1000 °C for one hour. The melts were quenched by removing the platinum crucible from the furnace and cooling briefly in air. The clear glassy samples were then powdered and stored under dry N_2 to minimize absorption of water. X-ray powder diffraction was used to verify the glassy nature of these samples.

3.2. NMR Methods

Nuclear magnetic resonance spectra were obtained using a home-built spectrometer in conjunction with an 8.4 T magnet (^{11}B Larmor frequency of 115.6 MHz). All spectra have been referenced to $Et_2O \cdot BF_3$. Static and magic angle spinning (MAS) NMR spectra were collected with a single pulse-acquire sequence using short pulse lengths, typically 2.4 μsec, and repetition times on the order of 2 s ($>5\,T_1$). The spectra were obtained with signal averaging of 64 scans.

3.2.1. Double Rotation NMR

Double rotation (DOR) NMR spectra of B_2O_3 glass were obtained on natural abundance samples using a commerical DOR NMR probe (Chemagnetics). A silicon nitride rotor with approximately 0.2 mL sample volume was packed with the powdered glass, and spun at values typically in the range of 3–4 kHz. The outer rotor frequency was chosen between 600 and 750 Hz. The sample spinning was stable (± 30 Hz) for several hours. NMR data was collected using a single pulse experiment, Fig. 1 a, by averaging 320 acquisitions with 1.5 s recycle delay between scans. Several DOR NMR spectra were collected at different outer rotor frequencies in order to distinguish the isotropic resonances from the spinning sidebands. The data were processed using 50 Hz line broadening.

3.2.2. Dynamic Angle Spinning NMR

Dynamic angle spinning (DAS) NMR spectra were obtained using 90% ^{10}B-enriched B_2O_3 and potassium borate glasses, in conjunction with a commercial DAS probe (Doty Scientific). Isotope depletion in these samples is necessary to quench spin diffusion, so that the magnetization may be stored during the rotor switch to the second spinning angle [14, 15]. A silicon nitride rotor with approximately 0.5 mL sample volume was packed with powdered sample, and spun at a frequency in the range of 5–7 kHz. Spinning under these conditions was stable for very long times (± 30 Hz, multiple days) The rotor orientation and pulse sequence for this experiment are shown in Figure 1 b.

The pure B_2O_3 experiments consisted of 160 scans at each of 96 delay times, with 3 s between scans to allow for proper relaxation. The DAS NMR spectra of potassium borate glasses were acquired with 64 to 128 acquisitions at each of 80 delay values with 15–60 seconds between scans to allow for full relaxation of all sites. The time required to obtain DAS NMR spectra under these conditions was approximately 24 hours for B_2O_3 and 24–96 hours for the modified samples. In all cases the angles $\phi_1 = 37.38°$ and $\phi_2 = 79.19°$ were used, with 40 msec for rotor axis switching and stabilization at the second angle. For this angle pair the echo forms after equal evolution time at both angles. The final π pulse is used to ensure acquisition of both the full echo and full anti-echo, and the data were collected as a hypercomplex set [12]. The DAS data was processed by Fourier-transforming the second time dimension, applying a shear transformation of 45°, followed by Fourier-transformation of the first time dimension and scaling of the corresponding frequency axis by 1/2 (see [12, 16]). All DAS NMR data were processed without smoothing. Isotropic spectra were obtained by projecting the entire two-dimensional data set onto the isotropic shift axis.

3.2.3. MQ-MAS

Isotropic spectra of ^{11}B in natural abundance glassy B_2O_3 were also obtained using the triple quantum-single quantum correlation experiment described recently by Frydman and Harwood [13]. The pulse sequence is shown in Figure 1 c. In this experiment, the sample is spun rapidly about a single axis, preferably the magic angle. We used a commercial DAS probe set to 54.74° by careful calibration with KBr. A silicon nitride rotor with 0.5 mL sample volume was packed with powdered sample and spun at a frequency typically chosen between 6 and 7 kHz.

The pulse sequence for MQ-MAS consists of three $\pi/2$ pulses, as shown in Fig. 1 c, which were 2.4 μsec in length. The first two pulses prepare triple quantum coherence, and the fixed delay Δ is chosen to be roughly the inverse of the quadrupole frequency, ω_Q^{-1}. We used $\Delta = 10$ μsec. The triple quantum coherence evolves for time t_1, and is then converted to single quantum coherence for detection. For spin 3/2, the isotropic echo forms at time (7/9) t_1 in the second time dimension, for any given t_1 (cf. standard DAS, where it appears at exactly t_1). To process the data we transform with respect to t_2, shear by arctan (7/9), transform with respect to t_1, and scale the isotropic frequency axis by 9/16. This sequence of processing steps, which occurs in any two-dimensional experiment for which part of the evolution time occurs after the mixing interval, is discussed in detail in [16].

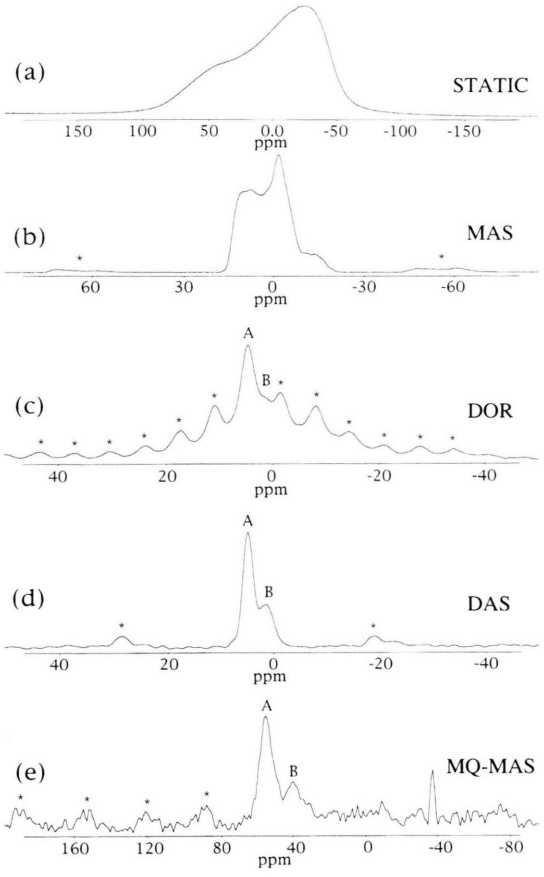

Fig. 2. One dimensional NMR spectra of ^{11}B in glassy B_2O_3 using different experimental techniques. (a) static powder pattern, (b) magic angle spinning at 6.5 kHz, (c) double rotation, (d) dynamic angle spinning, and (e) the MQ-MAS experiment. DAS NMR data were obtained using a 90% boron-10 enriched sample. All other spectra were obtained with natural abundance boron samples. Spinning sidebands are denoted by asterisks, while the two boron sites are labeled A and B. Peak A is the boroxol ring site, and peak B is the nonring BO_3 site. All shifts are relative to $Et_2O \cdot BF_3$.

We used a phase cycle consisting of 60° steps for the first pulse, with the second pulse leading and lagging by 180°; the third pulse was cycled independently through 45° steps. This yields a 96 step cycle, which showed good performance in rejecting artifacts. 480 scans were collected at each of 200 delay times, with 500 ms between scans. Due to the fast repetition of pulses (on the order of T_1), 96 dummy scans preceded each experiment. The total time for acquiring a two-dimensional MQ-MAS data set was approximately 16 hours.

4. Results

Various one-dimensional NMR spectra of ^{11}B in glassy B_2O_3 are shown in Figure 2. Results from standard methods such as static NMR and MAS NMR are compared with isotropic spectra obtained with double rotation, dynamic angle spinning and MQ-MAS NMR methods. A two-dimensional DAS NMR result for glassy $0.15\ K_2O \cdot 0.85\ B_2O_3$ is given in Figure 3. Included with the contour plot are the isotropic projection of the data set and anisotropic slices through the isotropic shifts of the three boron sites in this glass. Figure 4 shows the isotropic projections of several DAS NMR spectra from borate glasses with differing amounts of potassium oxide modifier.

5. Discussion

Figure 2 shows that all three methods used here, DOR, DAS, and MQ-MAS, provide significant resolution enhancements over conventional MAS. All show resolution of the ring and nonring boron sites in B_2O_3 glass, although these sites differ in quadrupole interaction magnitude by less than 5% and in chemical shift by only 5 ppm [14, 17]. DAS and MQ-MAS in particular show good resolution of these sites, with DAS having the better signal-to-noise. The resolution of DOR suffers from the large number of spinning sidebands, which arise from the relatively slow outer rotor speed. Synchronizing the outer rotor to the pulse sequence affords an effective doubling of the rotor frequency [18, 19], but we did not implement that feature here. The sideband problem for DOR is especially serious for disordered materials, as this one, because of the residual linewidths.

The peak dispersion behavior of MQ-MAS is different from DOR and DAS, as can be seen from (6) and (7) and Table 1. In DOR and DAS the quadrupole contribution to the isotropic shift is always negative, while in MQ-MAS it is positive for spin-3/2 and negative for spin-5/2. The chemical shift value can of course be positive or negative. For spin-3/2 it is added in all three of the experiments considered here, while for spin-5/2 it is subtracted in the MQ-MAS experiment. The resolution of the different experiments depends on the relative sizes and distributions of the quadrupole and chemical shift terms. For example, in B_2O_3 the boroxol ring boron have the larger quadrupole interaction and chemical shift relative to the non-

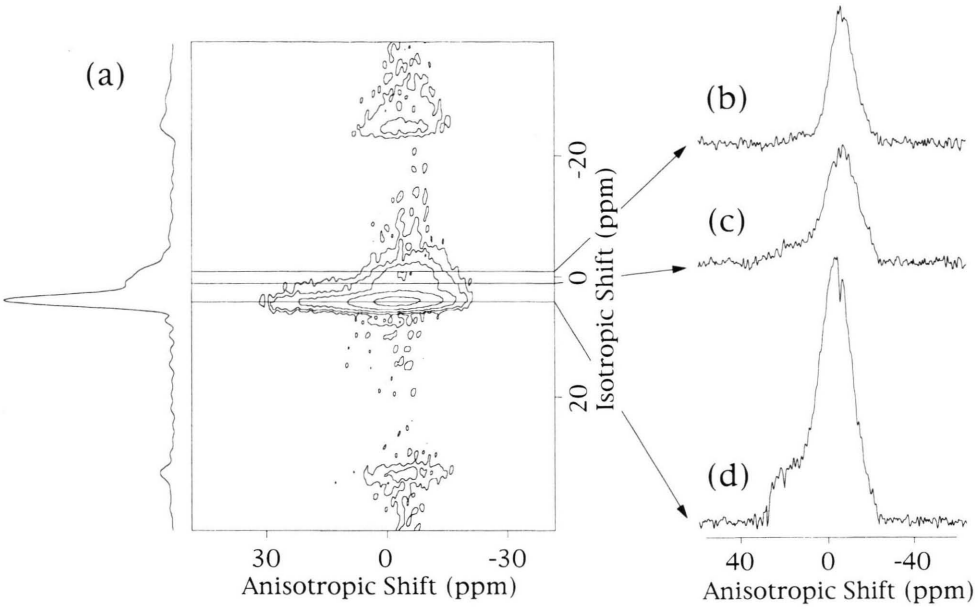

Fig. 3. Two dimensional DAS NMR spectrum of ^{11}B in 0.15 $K_2O \cdot 0.85\ B_2O_3$ glass at 8.4 T. These glasses are depleted in ^{11}B to 10%, in order to quench spin diffusion. Shifts are relative to $Et_2O \cdot BF_3$. (a) 2D-contour plot with isotropic projection. The contours at ± 30 ppm are spinning sidebands. (b) Slice at -0.2 ppm, the isotropic shift of the four-coordinate boron site. (c) Slice at 1.2 ppm, the non-ring BO_3 isotropic shift. (d) Slice 4.7 ppm, the isotropic shift of the boroxol ring boron.

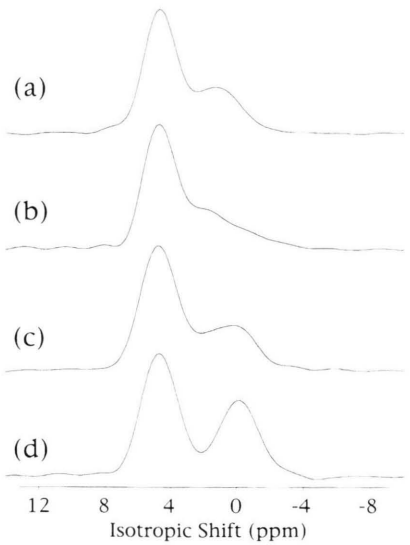

Fig. 4. Isotropic shift spectra of ^{11}B in $(K_2O)_x(B_2O_3)_{1-x}$ glasses, from DAS NMR. (a) $x=0.0$ (glassy B_2O_3). (b) $x=0.10$. (c) $x=0.20$. (d) $x=0.30$. Shifts are relative to $Et_2O \cdot BF_3$.

Table 2. Measured and calculated isotropic shifts, in ppm, for the three high-resolution NMR experiments. Calculated values are based on (6) and (7), using e^2Qq/h, η, and isotropic chemical shift as extracted from a series of DAS experiments performed in multiple fields.

Expt.	Ring boron		Nonring boron	
	Measured	Calc.	Measured	Calc.
DOR	4.6	4.2	1.5	0.2
DAS	4.6	4.2	1.0	0.2
MQ-MAS	54.7	55.5	39.5	43.7

ring boron (2.7 MHz and 18 ppm compared to 2.6 MHz and 13 ppm). In DOR and DAS the shifts due to these interactions oppose each other, while in MQ-MAS they add together and are amplified relative to DOR and DAS. Thus for these sites the MQ-MAS experiment gives much better peak separation than does DOR or DAS, as noted in Table 2. For spin-5/2 nuclei, such as oxygen-17 and aluminum-27, the dispersion is decreased substantially compared to DAS and DOR: by 45% for the chemical shift, and by 68% for the quadrupole coupling. For positive chemical shifts, however, the isotropic shift is still the sum of the two effects (with an overall minus sign), while in

DAS and DOR it is the difference of the shift contributions. Resolution of different sites is also influenced by the distributions of the interactions, as these and hence the linewidths are scaled differently in the various experiments.

We note as well that the differing dispersion provides a method to determine the chemical shift and quadrupole parameters separately. Currently this is best done by performing DAS or DOR in different magnetic fields and comparing the isotropic shifts. One could also, however, do MQ-MAS and DAS or DOR in the same field and use the differing isotropic shifts to solve for the chemical shift and the quadrupole product. Since probes are cheaper than magnets, this route seems the most economical.

More problematic than the spectral resolution is the amplitude resolution. For DOR the overlapping sidebands render full simulation of both the isotropic peaks and the sidebands necessary to estimate the relative isotropic peak intensities (see for example [20]). On the other hand, we have found DAS to be more sensitive than DOR to the differing nutation behavior of sites with differing quadrupole interactions. It is important to insure that all sites are in the limit of strong radiofrequency excitation. This is simple for B_2O_3, for example, but more difficult for modified borates where the four-coordinate boron has a much smaller quadrupole interaction than the three-coordinate sites. To check the reliability of intensities in this case, we perform DAS on crystal samples of known structure [15]. The nutation problem is particularly severe for the MQ-MAS experiment, where uneven excitation of the triple-quantum coherence will lead to an isotropic spectrum that is not representative of the relative site populations. In B_2O_3, where the two sites have similar quadrupole interactions, the relative intensities are in the correct ratio (Figure 2). However, in modified borates where the four-fold coordinate boron site has a much smaller quadrupole interaction than the three-fold sites [21], we have been unsuccessful in resolving both types of sites with MQ-MAS. This is likely due to nonuniformity in the multiple quantum excitation.

While we have shown that all three experiments are capable of resolving similar sites, even in a relatively disordered sample, the information content of the methods is different. The primary difference is between DOR and the other two methods, because DOR is not inherently two-dimensional. In DAS and MQ-MAS, correlations between coherences evolving under different effective Hamiltonians are detected, while in DOR all averaging is accomplished simultaneously. DOR yields a simple one-dimensional spectrum (complicated as noted by the spinning sidebands), which is ideal for determining the number of different sites and their isotropic shifts. DAS and MQ-MAS are inherently two-dimensional, in contrast, and the second dimension contains a great deal of information that is absent from a DOR spectrum. A two-dimensional DAS spectrum is shown in Figure 3. In this implementation the second dimension contains the spectrum of the sample spinning at the second DAS angle, 79.19° in this instance. This spectrum is ordered by the isotropic shift dimension, yielding a 79.19° spinning powder pattern for the sample as a function of the isotropic shift. Thus it is possible by taking slices of the two dimensional data set to extract the powder pattern of the spins with a given isotropic shift, say corresponding to one of the peaks in the isotropic dimension. From the shape of such a slice the quadrupole parameters can be estimated and the site assigned. Figure 3 demonstrates this procedure for three different boron sites in a potassium borate glass: the three-fold coordinated boron in boroxol rings, and not in rings, and the four-fold coordinated boron. These are assigned from their differing powder patterns and intensities. The disadvantage of acquiring the data while rotating off the magic angle is that both chemical shift anisotropy (CSA) and quadrupole anisotropies affect the lineshape. In ^{11}B CSA is small and can be neglected. In DAS this problem can be circumvented entirely by adding a second rotor hop to the magic angle, although this necessitates a second storage period and concomitant loss of signal. MQ-MAS should be free from this limitation, as the rotor always spins at the magic angle. The current triple quantum excitation and mixed phase behavior of the pulse sequence, however, do not give accurate anisotropic lineshapes.

Figure 4 shows the isotropic shift spectra, obtained with DAS, of a series of $(K_2O)_x(B_2O_3)_{1-x}$ glasses, as a function of added modifier. This figure demonstrates the power of high-resolution solid state NMR in following chemical changes, even in disordered materials. In these spectra it is clear that the boroxol ring boron peak is essentially unaffected by the added modifier, while the nonring boron peak diminishes in intensity. The new peak that appears is due to four-coordinate boron, which is the chemical product of modification [21]. The DAS experiment gives sufficient resolution to permit observation of this process in detail.

We have verified the precision of the intensity determinations of these spectra with DAS spectra of crystalline potassium borate samples. The data indicate that the boroxol rings are not modified by the added potassium oxide, until all nonring boron are exhausted. Details of these measurements, including DAS NMR, crystal studies, and Raman spectroscopy, will be published elsewhere [22].

6. Conclusions

All three of these experiments, DOR, DAS, and MQ-MAS, have significant potential as tools for measuring quadrupole interactions and thus solid state structure. In the case of DOR and DAS there are increasing numbers of applications [1]; the new MQ-MAS experiment [13], due to its ease of mechanical implementation, should be at least as popular.

We find that, while all three experiments work at least adequately for the realistic test case of resolving the boron sites in B_2O_3 glass, there are a number of reasons to prefer either DAS or MQ-MAS over DOR. Both of the former are easier to implement mechanically, MQ-MAS in particular requiring only a standard MAS probe and good phase-shifting in the spectrometer. The spinning sideband limitation is serious for DOR, especially with stronger interactions and disordered materials; the spinning speeds attainable routinely in DAS and MQ-MAS are as much as a factor of 10 greater, and more stable over longer times. DAS and MQ-MAS have higher information content, being inherently two-dimensional: they provide powder patterns for each site, and thus a route to obtaining η in addition to the quadrupole product $(e^2qQ/h)\sqrt{1+\eta^2/3}$. This is a valuable addition in structural studies (see for example [23]). MQ-MAS has the additional advantage over DAS of spinning at the Magic Angle, thus avoiding the storage time necessary in DAS during the rotor axis switch. The current most serious limitation of DAS is the storage time, which limits its applicability to samples with spin diffusion and T_1 times of the order of 50–100 msec or more. This prevents DAS from being used in a number of cases, for example for the study of aluminum in most samples, and for certain examples of heteronuclear coupling such as ^{17}O in the presence of aluminum or boron. At present the anisotropic lineshapes in MQ-MAS are inferior to those from DAS, but the phase characteristics of this experiment are not yet ideal. More troublesome is the poor signal-to-noise in MQ-MAS, which stems from the inefficient triple-quantum excitation currently employed. The triple-quantum excitation also appears to be uneven in exciting sites with differing quadrupole interactions. The advantage enjoyed by DOR in this respect is that, as a single-pulse experiment, it is relatively efficient in terms of spectrometer time and has good nutation behavior.

The high resolution afforded by these experiments has significant benefits for structural chemistry. All three offer the possibility of measuring quadrupole and chemical shift parameters with good precision, as we showed here with DAS as a probe of $(K_2O)_x(B_2O_3)_{1-x}$ glasses. We could follow in detail the modification of the boron oxide network upon addition of the alkali oxide modifier. This is an example of how these methods provide an attractive alternative to other methods of structure determination.

Acknowledgements

We thank Michael Janicke and Professor Bradley Chmelka for assistance with the double rotation experiments, and Professors Lucio Frydman and Philip Grandinetti for helpful discussions. U. W.-Z. acknowledges the support of the Petroleum Research Fund under grant 24396-AC4. This research was supported by the National Science Foundation under Grants No. DMR-9115787 and DMR-9508625.

[1] B. F. Chmelka and J. W. Zwanziger, Solid-state NMR line narrowing methods for quadrupolar nuclei: Double rotation and dynamic-angle spinning, in NMR Basic Principles and Progress, edited by B. Blümich and R. Kosfeld, Vol. 33, pp. 79–124, Springer, Berlin 1994

[2] M. Goldman, P. J. Grandinetti, A. Llor, Z. Olejniczak, J. R. Sachleben, and J. W. Zwanziger, J. Chem. Phys. **97,** 8947 (1992).

[3] U. Haeberlen, High Resolution NMR in Solids: Selective Averaging, volume Supplement 1 of Advances in Magnetic Resonance, Academic Press, New York 1976.

[4] C. Jäger, Satellite transition spectroscopy of quadrupolar nuclei, in NMR Basic Principles and Progress, edited by B. Blümich and R. Kosfeld, Vol. 31, pp. 135–170, Springer, Berlin 1993.

[5] L. van Wüllen, W. Müller-Warmuth, D. Papageorgio, and H. J. Pentinghaus, J. Non-Crystalline Solids **171,** 53 (1994).

[6] A. Samoson, E. Lippmaa, and A. Pines, Mol. Phys. **65,** 1013 (1988).

[7] A. Samoson and A. Pines, Rev. Sci. Instrum. **60,** 3239 (1989).

[8] A. Samoson, B. Sun, and A. Pines, New angles in motional averaging, in Pulsed Magnetic Resonance: NMR, ESR, and Optics, edited by D. M. S. Bagguley, Oxford University Press, Oxford 1992.
[9] A. Llor and J. Virlet, Chem. Phys. Lett. **152,** 248 (1988).
[10] B. F. Chmelka, K. T. Mueller, A. Pines, J. F. Stebbins, Y. Wu, and J. W. Zwanziger, Nature London **339,** 42 (1989).
[11] K. T. Mueller, B. Sun, G. C. Chingas, J. W. Zwanziger, T. Terao, and A. Pines, J. Magn. Reson. **86,** 470 (1990).
[12] P. J. Grandinetti, J. H. Baltisberger, A. Llor, Y. K. Lee, U. Werner, M. A. Eastman, and A. Pines, J. Magn. Reson. **A103,** 72 (1993).
[13] L. Frydman and J. S. Harwood, J. Amer. Chem. Soc. **117,** 5367 (1995).
[14] R. E. Youngman and J. W. Zwanziger, J. Non-Crystalline Solids **168,** 293 (1994).
[15] R. E. Youngman and J. W. Zwanziger, J. Amer. Chem. Soc. **117,** 1397 (1995).
[16] P. J. Grandinetti, Y. K. Lee, J. H. Baltisberger, B. Sun, and A. Pines, J. Magn. Reson. **A102,** 195 (1993).
[17] S. J. Gravina and P. J. Bray, J. Magn. Reson. **89,** 515 (1990).
[18] A. Samoson and E. Lippmaa, J. Magn. Reson. **84,** 410 (1989).
[19] Y. Wu, B. Sun, and A. Pines, J. Magn. Reson. **89,** 297 (1990).
[20] R. E. Youngman, S. T. Haubrich, J. W. Zwanziger, M. T. Janicke, and B. F. Chmelka, Science **269,** 1416 (1995).
[21] P. J. Bray, S. J. Gravina, D. H. Hintenlang, and R. V. Mulkern, Magn. Reson. Rev. **13,** 263 (1988).
[22] R. E. Youngman and J. W. Zwanziger, Network modification in potassium borate glasses: Studies with NMR and Raman spectroscopies, in preparation.
[23] I. Farnan, P. J. Grandinetti, J. H. Baltisberger, J. F. Stebbins, U. Werner, M. A. Eastman, and A. Pines, Nature London **358,** 31 (1992).